Early neuropathology of somatostatin/NPY GABAergic cells in the hippocampus of a PS1 × APP transgenic model of Alzheimer's disease

Blanca Ramos [a1], David Baglietto-Vargas [b1], Juan Carlos del Rio [a1], Ines Moreno-Gonzalez [b1], Consuelo Santa-Maria [a], Sebastian Jimenez [a], Cristina Caballero [a], Juan Felix Lopez-Tellez [b], Zafar U. Khan [c], Diego Ruano [a], Antonia Gutierrez [b], Javier Vitorica [a]

Affiliations:

[a]Department Bioquimica, Bromatologia, Toxicologia y Medicina Legal, Facultad de Farmacia, Universidad de Sevilla, 41012 Sevilla, Spain

[b]Department Biologia Celular, Genetica y Fisiologia, Facultad de Ciencias, Universidad de Malaga, Malaga, Spain

[c]CIMES/Department Medicina, Facultad de Medicina, Universidad de Malaga, Malaga, Spain

[1]Authors contributed equally to this work

* Corresponding Author:

Javier Vitorica
Dept. Bioquímica, Bromatología, Toxicología y Medicina Legal
Facultad de Farmacia, Universidad de Sevilla
41012, Sevilla, España
Tel: +34 952133344
Fax: +34 952233765
Email: vitorica@us.es

** Corresponding Author:

Antonia Gutiérrez Pérez, PhD
Departamento Biología Celular, Genética y Fisiología
Facultad de Ciencias, Universidad de Málaga
Campus Teatinos 29071, Málaga, España
Tel: +34 952133344
Fax: +34 952233765
Email: agutierrez @uma.es

Keywords: Alzheimer's disease**,** Neurodegeneration**,** Transgenic mice**,** Biomarkers**,** Hippocampus**,** Interneurons**,** Cholinergic**,** Glutamatergic, GABAergic

Abstract

At advanced stages, Alzheimer's disease (AD) is characterized by an extensive neuronal loss. However, the early neurodegenerative deficiencies have not been yet identified. Here we report an extensive, selective and early neurodegeneration of the dendritic inhibitory interneurons (oriens-lacunosum moleculare, O-LM, and hilar perforant path-associated, HIPP, cells) in the hippocampus of a transgenic PS1 × APP AD model. At 6 months of age, from 22 different pre- and postsynaptic mRNA markers tested (including GABAergic, glutamatergic and cholinergic markers), only the expression of somatostatin (SOM) and NPY neuropeptides (O-LM and HIPP markers) displayed a significant decrease. Stereological cell counting demonstrated a profound diminution (50–60%) of SOM-immunopositive neurons, preceding the pyramidal cell loss in this AD model. SOM population co-expressing NPY was the most damaged cell subset. Furthermore, a linear correlation between SOM and/or NPY deficiency and Abeta content was also observed. Though the molecular mechanism of SOM neuronal loss remains to be determined, these findings might represent an early hippocampal neuropathology. Therefore, SOM and NPY neuropeptides could constitute important biomarkers to assess the efficacy of potential early AD treatments.

1. Introduction

Alzheimer's disease (AD) is the most common neurological disorder affecting predominantly individuals over age 65. Patients with AD show a loss in memory and a decrease in their cognitive abilities. These changes are due to the progressive dysfunction and death of nerve cells that are responsible for the storage and processing of information. The pathological hallmarks of AD are beta amyloid (Abeta) deposits and plaques, hyperphosphorylation of tau and formation of neurofibrillary tangles, degeneration of synapses and loss of neuronal cells [52], [53], [39], [44].

A relatively high number of PS1, APP or PS1 × APP transgenic (tg) mice has been generated as valuable models of AD [23]. These tg mice models reproduce some but not all aspects of the disease. In this sense, APP or PS1 × APP tg mice displayed Abeta accumulation, neuritic alteration and behavioral and cognitive deficiencies but not the massive neuronal loss characteristic of the human disease [23], [2]. The apparition of Abeta depositions clearly precedes the decrease in the pyramidal cell number [43]. The reasons for these discrepancies are actually unknown, however, it is plausible that the different neuronal populations displayed a different vulnerability to the Abeta depositions. Therefore, the objective of this work was to establish whether specific GABAergic neuronal populations might be particularly vulnerable at early ages in the hippocampus of tg models.

The possible implications of the GABAergic system in the pathological evolution of these tg models have never been extensively evaluated, despite that GABAergic neurons constituted the major inhibitory system in the Central Nervous System. In this sense, we have previously observed a preferential vulnerability of the hippocampal GABAergic system during normal aging (see below).

Thus, in this work we have focused on hippocamapl somatostatin (SOM) and NPY expressing interneurons (oriens-lacunosum moleculare, O-LM, and hilar perforant path-associated, HIPP, cells) for four main reasons. First, the loss of SOM and/or NPY in AD patients is a well-reproduced observation. In this sense, the existence of a reduction in the number of cortical SOM/NPY immunopositive cells [13], [11], the SOM/NPY content in diverse brain areas [14] and in cerebrospinal fluid [37] has been described. In fact, as mentioned by Saito et al. [42], SOM is one of the few transcripts (0.5%) that consistently reduced in aged human brains (see also ref. [31]). Second, as mentioned above, we have previously observed that the hippocampal GABAergic system [41] and, in particular, the SOM interneurons were primarily affected during normal aging [49], the major risk factor in AD. Third, the APP and/or PS1 × APP tg models are hyperactive [48], [17], displaying disturbed activity patterns similar to those induced by the GABAergic inhibition [4]. Four, at the hippocampal formation, the SOM and NPY neuropeptides were principally co-expressed by the O-LM (in CA fields) and the HIPP cells (in the dentate gyrus) interneurons [19], [36]. Importantly, the O-LM and HIPP interneurons constituted a highly vulnerable cell population to several different insults and conditions. In this sense, these interneurons were preferentially affected in several models of temporal lobe epilepsy [8], [9], [12], [15], also sensitive to ischemic conditions [20].

On the other hand, this interneuronal subset is the major GABAergic population innervating the distal dendritic arbor of pyramidal and granular neurons [34], fired rhythmically at theta frequency [28], [29] and may regulate dendritic integration and plasticity [22]. In this sense, it has been demonstrated the implication of SOM neuropeptide in the acquisition of spatial maps and learning induced by novel environments [3]. Thus, the high cellular vulnerability together with its implication in memory processes makes this particular neuronal population a good candidate to be preferentially affected at early stages of the AD and in AD models.

Therefore, in this work we have evaluated whether the interneuronal population containing SOM/NPY was preferentially affected in transgenic models of Alzheimer's disease. We have thus studied the mRNA expression (using quantitative RT-PCR) and the neuronal density (using stereology) of this interneuronal population in a double tg model (PS1 × APP mice). This previously characterized tg model [6], [43] over-expressed the mutated form of human PS1 (PS1M146L) and human APP (APP751 with both the Swedish and London mutations; SL) proteins and developed Abeta depositions at early ages (3–4 months).

2. Methods

2.1. TG mice

The generation and initial characterization of the PS1 and PS1 × APP tg mice has been reported previously [6]. PS1 tg mice (C57BL/6 background) over-expressed the mutated PS1M146L form under the control of the HMGCoA-reductase promoter. PS1 × APP double tg mice (C57BL/6 background) were obtained by crossing homozygotic PS1 tg mice with heterozygotic Thy1-APP751SL mice (Transgenic Alliance). Mice represented F6–F10 offspring of heterozygous tg mice. Non-transgenic mice of the same genetic background were used as controls.

Anesthetized male mice were killed by decapitation and both hippocampi were dissected, frozen in liquid N_2 and stored at −80 °C until use. All animal experiments were performed in accordance with the guidelines of the Committee on Animal Research of the University of Seville.

2.2. RNA and protein extraction

Total RNA and proteins were extracted using the Tripure™ Isolation Reagent (Roche), according to the instructions of the manufacturer. This procedure allows the isolation of total RNA, DNA and protein fractions from a single sample. The contaminating DNA in the RNA samples was removed by incubation with DNAase (Sigma–Aldrich) and confirmed by PCR analysis of total RNA samples prior reverse transcription (RT). After isolation, the integrity of the RNA samples was assessed by agarose gel electrophoresis. The yield of total RNA was determined by measuring the absorbance (260/280 nm) of ethanol precipitated aliquots of the samples. The recovery of RNA was comparable in all groups (1.2–1.5 μg/mg of tissue).

In order to analyze the protein fraction, the protein pellets obtained using the Tripure™ Isolation Reagent were resuspended in 4% SDS and 8 M urea in 40 mM Tris–HCl, pH 7.4 and rotated overnight at room temperature. The total recovery and integrity of these fractions were determined by Lowry et al. [30] and SDS-PAGE.

2.3. RT-competitive PCR and real-time PCR

The retrotranscription (RT) was done using random hexamers, 3 μg of total RNA as template and either Ready-To-Go™ You-Prime First-Strand Beads (Amersham) or High-Capacity cDNA Archive Kit (Applied Biosystems) following the manufacturer's recommendations. After RT, the cDNA was purified using Microcon PCR cartridges (Millipore) and quantified by measuring the absorbance at 260/280 nm.

Competitive PCR was performed basically as described [41], [49]. Briefly, 100 ng of cDNA were mixed with increasing amounts of internal standards. Each sequence-specific internal standard was synthesized as described [50] and was different in size respect to their specific PCR product. The range of internal standard used was previously established in pilot experiments using control mice. After PCR (denaturation at 94 °C for 4 min and 32 cycles of 94 °C, 45 s, 60 °C for 45 s and 72 °C for 50 s followed by a final elongation period of 5 min at 72 °C), the PCR products were separated on a 1.7% agarose gel, photographed under UV illumination and films images were captured by a rotating scanner (Mustek Scan express 12.000 SP). The optical density (O.D.) of the competitor and target bands in individual lanes was determined (PCBAS 2.08) and the log ratio of amplified competitor to target fragments was plotted versus the log of the known amount of internal standard. Regression analysis and calculation of *x*-intercepts were done with the Sigmaplot 6.01 program.

For real time RT-PCR, each specific gene product was amplified using commercial Taqman™ probes, following the instruction of the manufactured (Applied Biosystems), using an ABI Prism 7000 sequence detector (Applied Biosystems). For each assay, a standard curve was constructed using increasing amounts of cDNA. In all cases, the slope of the curves indicated adequate PCR conditions (slope 3.2–3.4). The cDNA levels of the different mice were determined using two different housekeepers (i.e. GAPDH and beta-actin). The amplification of the housekeepers was done in parallel with the gene to be analyzed. Similar results were obtained using both housekeepers. Thus, the results were normalized using only the GAPDH expression.

In order to compare the results between both RT-competitive PCR and real time PCR, the data were normalized using the same standards and are expressed as relative units. Identical results were obtained using both competitive and real time RT-PCR (not shown), thus both approaches were used indistinctly.

2.4. Western blot

Western blots were performed as described previously [1]. Briefly, a total of 2.5 μg of hippocampal proteins were loaded on a 16% SDS-Tricine and transferred to a nitrocellulose (Hybond-C Extra, Amersham, Sweden). After blocking, the membranes were incubated overnight at 4 °C with the following primary antibodies: (i) monoclonal 6E10 (Sigma–Aldrich; dilution 1/100) and (ii) monoclonal anti beta-actin (Sigma–Aldrich; dilution 1/4000). Then, the membranes were incubated with an anti-mouse horseradish-peroxidase-conjugated secondary antibody (Dako, Denmark) at a dilution of 1/8000. The blots were developed using the ECL-plus detection method (Amersham, Sweden).

2.5. Tissue preparation

After deep anesthesia with sodium pentobarbital (60 mg/kg), 6-month-old control (WT), PS1 and PS1 × APP tg mice were perfused transcardially with 0.1 M phosphate-buffered saline (PBS), pH 7.4 followed by 4% paraformaldehyde, 75 mM lysine, 10 mM sodium metaperiodate in 0.1 M phosphate buffer (PB), pH 7.4. Brains were then removed, post-fixed overnight in the same fixative at 4 °C, cryoprotected in 30% sucrose, sectioned at 40 μm thickness in the coronal plane on a freezing microtome and serially collected in wells containing cold PBS and 0.02% sodium azide. Each experiment was composed of three to six sets of animals (each one containing one control, one PS1 tg mice and one PS1APP tg mice). All animal experiments were carried out in accordance with the NIH Guide for the care and use of laboratory animals and approved by the committee of animal use for research at Malaga University.

2.6. Immunocytochemistry

Sections that represented 1/7th of the total hippocampus from control and both tg mice (PS1 and PS1APP) were processed in parallel for light microscopy immunostaining using the same batches of solutions to minimize variability in immunocytochemical labeling conditions. Free-floating sections were first treated with 3% H_2O_2/3% methanol in PBS, pH 7.4 for 15 min to inhibit endogenous peroxidases, and with avidin-biotin Blocking Kit (Vector Labs, Burlingame, CA, USA) for 30 min to block endogenous avidin, biotin and biotin-binding proteins. For single immunolabeling sections were immunoreacted with one of the primary antibodies: anti-somatostatin (SOM) policlonal antibody (1:1000 dilution; Santa Cruz Biotechnology); anti-GAD67 monoclonal antibody (1:2500 dilution; Chemicon) or anti-Abeta monoclonal antibody 6E10 (1:1500 dilution; Sigma) overnight at room temperature. The tissue-bound primary antibody was then detected by incubating for 1 h with the corresponding biotinylated secondary antibody (1:500 dilution, Vector Laboratories), and then followed by incubating for 90 min with streptavidin-conjugated horseradish peroxidase (Sigma–Aldrich) diluted 1:2000. The peroxidase reaction was visualized with 0.05% 3-3′-diaminobenzidine tetrahydrochloride (DAB, Sigma–Aldrich), 0.03% nickel ammonium sulphate and 0.01% hydrogen peroxide in PBS. Sections were mounted on gelatin-coated slides, air dried, dehydrated in graded ethanols, cleared in xylene and coverslipped with DPX (BDH) mounting medium. Specificity of the immune reactions was controlled by omitting the primary antiserum.

For double immunoperoxidase SOM-NeuN labeling, sections were first immunostained for somatostatin as described above. After the DAB-nickel incubation (black reaction end product), sections were then washed and incubated overnight with anti-NeuN monoclonal antibody (1:1000 dilution), followed by 1 h incubation with anti-mouse biotinilated IgG antibody (1:500 dilution; Vector Laboratories), and 90 min incubation with streptavidin-conjugated horseradish peroxidase (Sigma–Aldrich) diluted 1:2000. This second immunoperoxidase reaction was developed with DAB only (brown reaction end product). Sections were finally mounted on gelatin-coated slides, air dried, dehydrated in graded ethanol, cleared in xylene and coverslipped with DPX (BDH mounting medium). Specificity of the immune reactions was controlled by omitting the primary antisera.

For double SOM/NPY immunofluorescence, labeling, sections were incubated with goat anti-SOM (1:1000) and with rabbit anti-NPY (1:5000; Sigma–Aldrich). Immunoreaction was visualized with Alexa 568 donkey anti-goat (1:1000 dilution, Molecular Probes) and

biotinylated donkey anti-rabbit (1:200; Amersham) and streptavidin-conjugated Alexa 488 (1:2000 dilution; Molecular Probes).

Sections were mounted onto gelatin-coated slides, coverslipped with 0.01 M PBS containing 50% glycerin and 2.5% triethylenediamine and then examined under a confocal laser microscope (Leica TCS-NT).

2.7. Stereological analysis

Immunopositive cells for SOM, GAD67 or NeuN, and cresyl-violet stained principal cells belonging to the different animal groups (WT, PS1 and PS1 × APP) (n = 3–6/group; 10–15 sections per animal) were quantified according to the optical fractionator method, using an Olympus BX51 microscope (Olympus, Denmark) interfaced with a computer and a color JVC digital videocamera. The CAST-Grid software package (Olympus, Glostrup, Denmark) generated sampling frames with a known area (a_{frame}) and directed the motorized X–Y stage (Prior proscan, Prior Scientific Instruments, Camba, UK), and a microcator (MT12, Heidenheim, Germany), which monitored the movements in the Z-axis with a resolution of 0.5 μm. The number of neurons was quantified in every seventh section (with a distance of 280 μm) through the entire antero-posterior extent of the hippocampus (between −0.94 mm anterior and 3.64 mm posterior to Bregman according to the atlas of Paxinos and Watson). This selection criteria prevented counting neurons from contiguous sections. An average of 10–15 serial sections was measured in each animal. One side of the entire hippocampus (CA1, CA2–3 and DG) was defined using a 4× objective and the number of neurons was counted using a 100×/1.35 objective. The number of counting frames (each one 1874.2 μm^2) varied with the hippocampal region or subfield layer analyzed. We used the optical 3 μm from de upper surfaces as look-up, and those 3–13 μm from the surfaces as reference sections. The numerical density (ND; cells/mm^3) of immunopositive cells was estimated using the following formula: $ND = N/(A \times 10\ \mu m/SV)$, where N is the number of dissector-counted somatic profiles, A the area and SV is the volumetric shrinkage factor of the sample (the SV was determined in the same way as described) [25], [26]. The area shrinkage factor (0.76–0.91) and the thickness shrinkage factor (0.45–0.56) were calculated according to the type of animal and age. For the principal cells, the software calculated the estimated total number of cresyl-violet stained nuclei in the CA1 region utilizing the optical fractionator formula, $N = 1/bsf \times 1/ssf \times 1/asf \times 1/hsf \times \Sigma Q^-$ [16], where bsf is the block sampling fraction, ssf represents the section sampling fraction, asf the area sampling fraction, which is calculated by dividing the area sampled with the total area of the layer, hsf stands for the height sampling fraction, which is calculated by dividing the height sampled (10 μm in this study) with the section thickness, and ΣQ^- is the total count of nuclei sampled for the entire layer.

The precision of the individual estimations is expressed by the coefficient of error (CE) [7] and here we have estimated the total CE (CE group value) that was calculated using the CEs in each individual animal. The CEs ranged between 0.01 and 0.03.

2.8. Hippocampal volume

We estimated the hippocampal volume of wildtype (n = 6) and PS1 × APP mice (n = 6) applying the Cavaliers principle in combination with point counting, a method which provides efficient and unbiased volume estimation:$V=a(p)\cdot d^{-}\cdot\sum i=1nPi$where '$a(p)$' is the

area associated with each sampling point, '$\bar{d}$' the mean distance between two consecutively studied sections and '$\sum i=1nPi$' is the sum of points hitting. From the complete rostrocaudal set of sections in each animal a 1:7 series was selected for analysis. An average of 10–12 sections was measured in each animal. The CE of the volume [7] ranged between 0.03 and 0.07. Data demonstrated the absence of differences between WT, PS1 and PS1 × APP mice (10.50 ± 0.84, 9.98 ± 0.93 or 9.93 ± 1.52 mm^3, $n = 6$, for WT, PS1 and PS1 × APP, respectively).

2.9. Lacunosum moleculare volume

The volume of the SOM-positive lacunosum moleculare layer in the CA1 subfield of wildtype ($n = 3$) and PS1 × APP ($n = 3$) mice was estimated according to the following formula: $V = A \times h$, where 'A' is the area of the layer and 'h' is the height of each section. From the complete rostrocaudal set of sections in each animal a 1:7 series was selected for analysis.

2.10. Statistical analysis

Data was expressed as mean ± S.D. The comparison between two mice groups (WT and PS1APP tg mice) was done by two-tailed *t*-test. For comparison between several groups (WT, PS1, APP and PS1APP mice) and ages, we used one-way ANOVA or multifactor ANOVA, followed by Scheffe post hoc multiple comparisons test (Statgraphics plus 3.1). The significance was set at 95% of confidence.

3. Results

3.1. Early reduction of hippocampal SOM and NPY neuropeptide mRNAs in PS1 × APP tg mice

We first determined the expression of SOM and NPY mRNAs in hippocampus from a large mice population (25–30 mice per group) and in a wide age range (2-, 4-, 6-, 12- and 18-month-old mice) of non-tg mice (WT), PS1 and PS1 × APP double tg mice. As compared with age-matched WT or PS1 mice (Fig. 1A and B), in PS1 × APP double tg mice the expression of both neuropeptides decreased significantly even at very early ages. At 4 months, a significant decrease ($-23.01 \pm 20.4\%$, $n = 26$; Scheffe $p < 0.05$) was observed in SOM expression whereas, at 6 months, both SOM and NPY mRNAs decreased significantly ($-33.63 \pm 18.2\%$ and -27.54 ± 17.2, $n = 30$, Scheffe $p < 0.01$, for SOM and NPY, respectively). The SOM and/or NPY expression in the double PS1 × APP tg mice displayed a further decrease at 12 months whereas, in WT and PS1 mice, the expression of these mRNAs was not significantly modified. These results indicated that, at early ages (from 4- to 12-month-old) there was a specific reduction in the expression of SOM and NPY in the PS1 × APP double tg mice. On the other hand, as expected from the known effect of aging in the expression of both neuropeptides [49], in older animals (18-month-old), a decrease was also observed in PS1 single tg mice.

It could be argued that the observed changes in both SOM and NPY expression were due to the over-expression of the wild type and/or mutated forms of PS1 and/or APP transgenes. Although we have not directly tested this possibility, it seemed unlikely since: (i) no differences in the SOM and NPY expression were observed in 2-month-old PS1 × APP tg mice, compared to WT mice and (ii) no differences were observed between PS1 and WT until 18 months.

On the other hand, it has been proposed that most of the NPY positive interneurons also express SOM [19], [36]. In fact (Fig. 1C), there was a highly significant linear correlation between both parameters. A reduced expression in SOM was accompanied by a parallel decrease in NPY expression. Interestingly, the age-dependent modifications on the expression of both neuropeptides, determined in WT and PS1 tg mice, also fit well with those observed in PS1 × APP mice. This parallel decrease in SOM and NPY expression indicated that the same neuronal population should be affected in the PS1 × APP tg mice. The expression of other GABAergic marker, such as parvalbumin, was not modified in the same PS1 × APP tg mice (Fig. 1C inset).

To further determine if the reduction in the SOM expression was specific of the PS1 × APP double tg mice, hemizygous PS1 mice were crossed with hemizygous APP mice. Thus, all four genotypes (WT, PS1, APP and PS1 × APP) were obtained in the first generation. At 6 months of age, as compared with WT or PS1 mice (Fig. 1D), the double PS1 × APP tg mice showed a significant decrease ($-30.9 \pm 9.1\%$, $n = 6$, Scheffe $p < 0.05$) in the SOM expression, similar to that showed previously. No differences were observed between PS1 tg mice and WT littermates. The expression of SOM mRNA in APP single tg mice displayed an intermediate reduction ($-14.8 \pm 10.8\%$, $n = 6$), although non significantly as compared with WT mice (Fig. 1D). Interestingly, the Abeta deposition was delayed in this single APP tg mice, as compared to double tg [6]. Thus, the decrease in SOM and/or NPY expression seems to be correlated with the severity of the pathology (Abeta depositions, see below) in these mice models.

3.2. The number of SOM immunoreactive cells is significantly decreased in PS1 × APP tg mice hippocampus at 6 months of age

We next tested if the observed reduction in the SOM mRNA was also accompanied by a decrease in the number of SOM expressing cells. We have thus combined specific immunohistochemical detection of interneurons, expressing SOM, with an unbiased stereological cell counting method in the hippocampus of PS1 × APP transgenic at 6 months of age.

The immunohistochemical study showed that the distribution of SOM-positive neurons in the hippocampus of WT and tg animals (Fig. 2) was comparable to previous reports. Most SOM-positive neurons were found in the stratum oriens (SO) of the CA1–3 subfields and in the hilus of dentate gyrus [36]. In addition, few SOM-positive cells were also found in statum lucidum of CA3 region. Occasionally, some immunoreactive cells were also seen in strata pyramidale and radiatum of CA1–3 regions.

A reduced number of SOM-positive cells throughout the hippocampus of PS1 × APP mice, when compared to the age-matched WT or PS1 mice, was clearly observed (see Fig. 2, C1–C2 versus A1–A2). In addition, the morphological examination showed the presence of dystrophic SOM-positive neurons or neurites in the double tg mice. However, no differences were detected between PS1 tg mice and control group (see Fig. 2, B1–B2 versus A1–A2).

The stereological quantification of SOM-positive cells in CA1–3 subfield and dentate gyrus of WT, PS1 and PS1 × APP mice ($n = 6$, 10–15 sections per animal; Fig. 2E) revealed a significant and pronounced reduction in the numerical density (cells/mm^3) of

SOM-positive cells in all regions of the hippocampus of PS1 × APP tg mice, in comparison with WT or PS1 mice. The number of SOM cells exhibited a 63.9 ± 4.6% decrease in CA1 (Scheffe $p < 0.05$); 52.5 ± 10.8% in CA2–3 regions (Scheffe $p < 0.05$) and 63.1 ± 5.9% in dentate gyrus hilus (Scheffe $p < 0.05$). However, the number of SOM interneurons remained unchanged between PS1 tg and WT mice. Furthermore, no differences between PS1 × APP tg mice and either WT or PS1 mice were observed at younger ages (2-month-old, not shown).

To determine the selective vulnerability of hippocampal interneurons containing SOM, we have counted striatal interneurons that express SOM using the same immunostained brain sections. The stereological analysis showed no significant differences between PS1 × APP and WT mice (1182 ± 69 cells/mm^3 versus 945 ± 104 cells/mm^3, 10–12 sections per mouse, $n = 3$; for WT and PS1 × APP, respectively).

On the other hand, stereological measurement of total pyramidal cell number, in hippocampal CA1 subfield of 6-month-old PS1 × APP tg mice, did not reveal any significant difference when compared to WT or PS1 mice (see Fig. 2E inset). Furthermore, no significant differences in the density of perisomatic inhibitory PV positive cells (not shown but see Fig. 2D1–3) were detected between the double tg and wild type mice.

3.3. SOM cells co-expressing NPY are the interneurons most severely affected in 6-month-old PS1 × APP mice hippocampus

As suggested by the parallel reduction in the SOM and NPY mRNA expression, the SOM and NPY positive GABAergic cells could be preferentially affected in PS1 × APP tg mice. Thus, we have analyzed the vulnerability of SOM/NPY subpopulation in PS1 × APP mice by double immunofluorescence labeling. Representative confocal images (from five different independent experiments) are shown in Fig. 3. Though we have not quantified the extent of this co-localization, numerous interneurons co-expressed both neuropeptides in stratum oriens of CA1 and hilus of dentate gyrus of WT (Fig. 3A3) and PS1 (Fig. 3B3) mice. The number of interneurons immunolabeled for NPY was highly reduced in PS1 × APP mice (Fig. 3C1) as compared with WT (Fig. 3A1) and PS1 groups (Fig. 3B1). The loss of NPY-positive cells correlates with the loss of SOM-positive cells as shown in the merged image (Fig. 3C3).

3.4. The decrease of SOM and NPY neuropeptides is highly selective at early ages in the hippocampus of PS1 × APP tg mice

The reduction in the expression of SOM and NPY could be specific or, on the other hand, reflecting a generalized modification in the GABAergic system. In order to analyze this point, using a new population of 6-month-old PS1 × APP tg mice ($n = 18$), we have quantified the expression of mRNAs considered as presynaptic and postsynaptic markers of this system (i.e. GAD65 enzyme, the neuropeptides cholecystokinine (CCK) and VIP; and the calcium binding proteins PV and Calbindin (Cb))[36]. The expression of SOM and NPY neuropeptides was included for comparative purposes. In parallel, we also quantified the expression of the major hippocampal alpha subunits of the $GABA_A$ receptor (alpha1, alpha2 and alpha5 subunits). The results are shown in Fig. 4A.

Concerning the interneuronal markers, only the expression of SOM and NPY displayed a significant reduction (−31.3 ± 17.9% or −34.7 ± 16.9%, $n = 18$, for SOM and NPY, respectively; two-tailed $t = 5.96$, $p < 0.0001$ and $t = 4.64$, $p < 0.0001$) as compared with WT mice. This reduction was similar to that observed in Fig. 1A, B and D. The absence of changes in the Cb expression was in contrast with the results reported by Palop et al. [38]. This apparent discrepancy could be due to differences in the onset of the pathological modifications between the different tg models used. On the other hand, at this age, the expression of the $GABA_A$ receptor subunits was not modified (see also ref. [40]).

In addition, using the same mRNA samples, we have also quantified the expression of synaptophysin and several specific markers of glutamatergic (AMPA receptor subunits) and cholinergic (muscarinic and nicotinic receptor subunits) systems (Fig. 4B). As shown, no differences were observed in any of the mRNAs quantified. The expression of the ChAT enzyme, determined in the basal forebrain, was also similar between control and PS1 × APP mice (Fig. 4B). These results emphasized the specificity and reproducibility in the observed SOM and NPY modifications at this age.

3.5. The decrease of SOM/NPY positive cells is a consequence of an early neurodegeneration of inhibitory interneurons in the hippocampus of PS1 × APP tg mice

To ascertain whether the reduction in the number of SOM-positive neurons in PS1 × APP mice reflects a diminution in the absolute number of interneurons or hypofunctionality with altered phenotype, we have performed parallel stereological counts of SOM-positive cells and total GABAergic population in the stratum oriens of CA1 using double SOM-NeuN immunostained sections. NeuN is a specific neuronal marker and, in the stratum oriens, most of the neurons are GABAergic [19], [36]. A comparison of the distribution of SOM/NeuN interneurons in the stratum oriens of CA1 between WT and PS1 × APP tg mice is shown in Fig. 5A and B. The density of SOM labeled cells as well as NeuN labeled cells was significantly reduced in PS1 × APP tg mice. The results of stereological quantification are shown in Fig. 5C. There was a marked reduction of SOM-positive cells (−61.8 ± 19.4%, $n = 4$; 10–15 sections per mouse) accompanied by a decline in the total NeuN positive population (−41.4 ± 7.9%, $n = 4$; 10–15 sections per mouse). This decrease was similar to that observed using anti-GAD67 immunolabeled sections (−46.3 ± 2.8%, $n = 3$, results not shown). Importantly, the loss in the SOM-positive cell number (5114 ± 695 cells/mm^3; calculated from the difference between WT and PS1 × APP) was similar to the loss of NeuN labeled cells (5893 ± 222 cells/mm^3; see Fig. 5C). This finding demonstrated a significant early loss of inhibitory interneurons that mostly correspond to the SOM-containing population in the hippocampus of PS1 × APP tg mice.

3.6. The SOM-immunolabeled axonal field in stratum lacunosum moleculare is reduced in 6-month-old PS1APP mice hippocampus

The SOM-immunostained stratum lacunosum moleculare (the axon terminal field of O-LM cells) of PS1 × APP mice showed an apparent shrinkage, when compared to WT animals (Fig. 6A and B). To investigate whether the loss of SOM-positive cells in the stratum oriens produces a diminished axonal field, we have measured the volume of this

layer in the CA1 region of PS1 × APP and control mice (Fig. 6C). The results revealed a generalized reduction in rostral, medial and caudal levels being statistically significant at the caudal level (−32.54 ± 6.91%, $n = 3$; 10–15 sections per mouse; two-tailed $t = 3.11$, $p = 0.04$). As a consequence, the total volume (rostral + medial + caudal) also showed a significant decrease (−28.02 ± 4.9%, $n = 3$; two-tailed $t = 3.87$, $p = 0.03$). Thus, the decrease in the SOM-positive cell number in PS1 × APP was also paralleled by a decrease in the innervated area. It is noteworthy that the decrease in the numerical density of SOM cells exceeded the reduction of the total axonal volume immunopositive for SOM (−63.9 ± 4.6% versus −28.02 ± 4.9%). This difference could indicate the existence of axonal sprouting of the remaining SOM-positive fibers.

3.7. The decrease in SOM and/or NPY neuropeptides is related to the Abeta content in 6-month-old PS1 × APP tg mice

As shown (Fig. 7C), the expression of the mRNA encoding for SOM displayed variability in the PS1 × APP tg mice. The SOM expression in some PS1 × APP individuals was identical to controls whereas a profound decrease was observed in other cases. Similar results were obtained for NPY mRNA expression (not shown). Thus, we have determined the Abeta content from 23 different 6-month-old PS1 × APP tg mice.

The total Abeta content was determined by Western blot, using the mAb 6E10. As shown in Fig. 7A, a major band of 4.5 kDa was detected using this approach. This 4.5 kDa band corresponded to the monomeric form of the Abeta peptide [51]. This band was also detected using the mAb WO2 (not shown) [24]. Other immunostained bands of higher molecular weight could be also observed at higher exposition times (dimeric and/or trimeric forms of Abeta, not shown) [51]. However, this approach did not resolve between Abeta 1–40 and 1–42 (not shown).

Fig. 7A showed a representative Western blot**.** As shown, the amount of 4.5 kDa band varied drastically between the different mice tested, from very low levels (animal #15) to high levels (#233 or #200). This high variability was not due to differences in the original protein loading (Fig. 7B). As shown (Fig. 7C), the expression of Abeta displayed high variability within the PS1 × APP population (similar to the SOM neuropeptide in the same mice population, Fig. 7C). We next plotted the mRNA levels of SOM and NPY versus the corresponding Abeta value, determined in the same animals. As shown in Fig. 7D, for both neuropeptides, there was a significant inverse linear correlation with the amount of Abeta peptide. Those PS1 × APP mice displaying low amount of Abeta content also showed high levels of both SOM and NPY mRNAs whereas those PS1 × APP mice with high content of Abeta peptides displayed low levels of both SOM and NPY neuropeptides.

In order to determine the intracellular/extracellular localization of Abeta in PS1 × APP tg model, we have performed immunostaining with 6E10 antibody in hippocampal sections of 2-, 4- and 6-month-old mice (Fig. 7E–G, respectively). The results showed intense immunolabeling of pyramidal cell bodies and proximal dendrites at all three ages tested. Extracellular deposition was first observed at 4 months old and increased with age. Abeta deposits were mainly located in stratum oriens of CA subfields (Fig. 7F and G) and hilus

of dentate gyrus (not shown). Interestingly, no intracellular Abeta expression was detected in the stratum oriens or in the hilus.

4. Discussion

We have recently demonstrated the existence of a significant deficit in the SOM/NPY GABAergic population in aged rat hippocampus [49]. Since aging is the main risk factor for AD, we investigated in this work whether this hippocampal interneuronal population was also preferentially affected in AD transgenic models. Our results clearly demonstrated the existence of a profound decrease in the expression of both SOM and NPY mRNAs in PS1 × APP mice, as early as 4–6 months of age, progressing towards lower values during the aging process. At this early period in the life span of the tg mice, no modifications were detected in any of the other GABAergic, glutamatergic or even cholinergic markers tested. Furthermore, this change was observed in absence of modifications in the expression synaptophysin (a presynaptic marker) or ChAT in the basal forebrain (a classical AD marker) [32]. Since SOM neuropeptide is implicated in both memory acquisition and Abeta degradation [3], [42], this selective loss could also represent one of the initial steps in the pathologic evolution of AD. Additionally, the expression of both neuropeptides could constitute a valuable tool to determine the efficacy of therapeutic treatments.

The decrease in the SOM and/or NPY content in AD cases was already known (see Section 1 and ref. [7]). However, here we demonstrate that this specific and early neurochemical alteration is associated to a reduced number of SOM-NPY interneurons in our PS1 × APP tg mice. In this respect, our results clearly probed the existence of a marked reduction (50–60%) in the numerical density of SOM immunopositive cells in CA1–3 stratum oriens and dentate gyrus of 6-month-old PS1 × APP tg mice. Furthermore, this reduction was not merely reflecting a modification in the phenotypic properties of this particular neuronal population (hypofunctional cells)[46]. The presence of SOM-positive dystrophic neurites indicated the existence of a neurodegenerative deterioration of this interneuronal population. Moreover, the SOM-NeuN double immunolabeling experiments clearly established that the decrease in the SOM immunopositive cell number was due to cell death. The SOM-positive cells were concentrated in the stratus oriens in the CA fields [36] and, in this layer, all neurons are GABAergic [19], [36]. Thus, the direct comparison between NeuN and SOM density in stratum oriens allowed us to discriminate between hypofunctionality and neurodegeneration. Importantly, our results demonstrated the existence of a similar, if not identical, decrease in both SOM and NeuN immunopositive cells in PS1 × APP tg mice (Fig. 5). In consequence, we conclude that the decrease in the SOM immunopositive cells was due to the neurodegeneration of this particular interneuronal population in the PS1 × APP tg mice. Importantly, in parallel experiments, the numerical density of either SOM in striatum, or hippocampal PV positive cells (not shown) and CA1 pyramidal cells remained unaltered (as compared with age matched WT or PS1 tg mice). It should be noted that, in this tg model, the decrease in the pyramidal cell number was observed in 17-month-old animals [43]. Thus, these data demonstrated the specific an early vulnerability of SOM expressing-population in the double PS1 × APP tg model.

On the other hand, in the hippocampus, at least three different subsets of SOM interneurons have been identified (i.e. apical projecting cells, O-LM and HIPP cells; medial septal projecting cells and bistratified cells). Most of the O-LM and HIPP cells coexpressed SOM and NPY whereas the septal projecting cells and the bistratified cells coexpressed SOM/Cb or SOM/PV, respectively [33], [19]. Our confocal and double labeling experiments suggested that SOM/NPY subpopulation decreased extensively. In fact, the molecular characterization also demonstrated a parallel reduction in both SOM and NPY mRNA expression (see Fig. 1). Taken together, the molecular and immunohistological experiments clearly demonstrated that the SOM-NPY interneuronal subset (mostly the O-LM and HIPP cells) was preferentially affected at early steps of the pathological evolution in PS1 × APP models. To the best of our knowledge, this is the first time that an early and neuron specific neurodegenerative process has been described in tg AD models. It is noteworthy that the O-LM and HIPP cells represent a major GABAergic population in the hippocampal formation comprising, approximately, 40–60% of the total inhibitory cells [27]. Thus, the decrease in the SOM cell density, observed in this work (50–60%), should constitute a substantial decline of the total GABAergic population in this brain area.

The reasons that determined this cell loss are unknown. However, our results also demonstrated the existence of an inverse correlation between the SOM/NPY expression and the Abeta content in the different PS1 × APP mice at 6 months of age. Further, this effect was also consistent with the gradual deficiency in the SOM expression observed between PS1, APP and PS1 × APP littermates (Fig. 1D). In this sense, the implication of Abeta is well established as one of the responsible factors for the pathological events that determined the neuronal death observed in AD [35]. However, it is unclear whether the toxic effects are due to intra- or extra-cellular Abeta (see ref. [54] for review). In this respect, the existence of an extensive pyramidal cell loss and the cognitive deterioration have been associated with the expression of intracellular Abeta peptides [10], [5]. We have also tested the possible expression of intracellular Abeta by the interneurons in the stratum oriens (see Fig. 6), yet, no immunostaining in these cells was observed in either 2-, 4- or 6-month-old PS1 × APP mice (even after formic acid treatment), whereas a prominent expression was detected in the pyramidal cell layer. Thus, in this particular case, the SOM expressing cells may be affected by extracellular, secreted Abeta peptides. The present results do not allow us to discriminate between a direct Abeta effect on the SOM/NPY interneurons or, on the contrary, an indirect Abeta cytotoxic effect on this neuronal population. Concerning to this latter possibility, the 4–6-month-old PS1 × APP mice develop an extensive inflammatory response with a substantial microglial activation and induction of, among other factors, TNF-alpha and iNOS expression (manuscript in preparation and ref. [6]). These factors could be implicated in the degenerative processes observed in the AD models (ref. [18] and references therein). These two alternatives are not mutually exclusive and we cannot exclude a synergic effect of both processes in the degeneration induced by the Abeta deposition.

On the other hand, our results also demonstrated that the reduction in SOM cell number was accompanied by a decrease in the corresponding immunoreactive axonal volume in the lacunosum moleculare field (see Fig. 6). The O-LM and HIPP neurons belong to the distal dendritic inhibitory cells, e.g. oriens/alveus interneurons with lacunosum moleculare axon arborization [45]. Therefore, this decrease suggested that, not only the

number of SOM cells, but also the number of inhibitory synapses at the distal apical dendrites were reduced in the PS1 × APP tg model.

The physiological consequences of the reduction in the SOM content, the total number and the innervated area of the SOM cells are actually unknown. However, the distal inhibitory cells played an essential role in the synaptic signal integration and input plasticity of principal cells [47], [21]. In fact, their axonal terminations were co-aligned with the perforant path input from the entorhinal cortex and the SOM-positive O-LM cells fired rhythmically at theta frequencies, contributing to the hyperpolarization of the principal cells [28], [29]. This rhythmic hyperpolarization could contribute to the de-inactivation of voltage-gated ion channels, facilitating somatodendritic back-propagation action potentials and synaptic plasticity of the principal cells [28], [29]. Thus, the profound (50–60%) and specific loss of SOM cells and their lacunosum moleculare innervation could be implicated, at least in part, in the memory impairment observed in AD tg models. On the other hand, the specific degeneration of the O-LM and HIPP cells in the PS1 × APP tg mice might produce an imbalance between excitation and inhibition on the distal dendritic tree, increasing the pyramidal excitability, similar to that observed in temporal lobe epilepsy models [12] and, in consequence, increasing the vulnerability of these cells,

Finally, it has recently been demonstrated the implication of SOM in the regulation of neprilysin activity at the neuronal surface and the degradation of Abeta peptides [42]. In fact, SOM upregulated the neprilysin activity transported to the plasmatic membrane and, in consequence, reducing the soluble Abeta deposition. Thus, the degeneration of the O-LM and HIPP cells, that determines the decrease in the expression of SOM neuropeptide, could also produce a diminution in the neprilysin activity. In consequence, this neurodegenerative process could contribute to the progressive age-dependent accumulation of Abeta peptides observed in both AD cases and tg models.

In sum, our findings demonstrate, for the first time, a substantial early loss of SOM and/or NPY GABAergic neurons from the hippocampus of double PS1 × APP tg mice. This selective modification was observed in absence of changes in other neuronal markers of GABAergic, glutamatergic and cholinergic systems or the principal cell number. This neurodegenerative process provides a cellular explanation to the decrease in the SOM neuropeptide expression (also observed in AD cases). Since SOM neuropeptide is implicated in the control of neprilysin activity, the loss of SOM neurons also explains the observed decrease in neprilysin activity and Abeta accumulation in the hippocampus. On the other hand, the SOM-NPY GABAergic neurons are implicated in the coordination of pyramidal cells activity, then, the early neurodegeneration of these interneurons could implicate a reduction in the synaptic plasticity of the principal cells and determine, at least in part, the deficits in memory/learning process observed in early phases of AD. Finally, the expression of both SOM and NPY mRNAs could be considered as specific and early molecular markers of AD in the PS1 × APP models. Thus, these neuropeptides could constitute important molecular tools to improve the assessment of the efficacy of potential AD treatments in this mice model.

Acknowledgments

We would like to thanks to Dr. J.A. Aguirre for his assistance with the stereological analysis and Aventis-Pharma for the transgenic mice models. This work was supported by grants SAF2002-03448 (to J.V.), FIS PI030214 (to A.G.), FIS PI030177 (to D.R.) and Aventis Grants (to J.V. and A.G.). D.R. and Z.U.K. were supported by a Ramon y Cajal program from Ministerio de Ciencia y Tecnologia. B.R. and J.F.L.-T. were recipients of fellowships from Ministerio de Ciencia y Tecnologia, and I.M.-G. and J.C.R., D.B.-V. from Fondo de Investigaciones Sanitarias and Junta de Andalucia, respectively.

References

[1] Araujo F, Tan S, Ruano D, Schoemaker H, Benavides J, Vitorica J. Molecular and pharmacological characterization of native cortical gamma-aminobutyric acid(A) receptors containing both alpha(1) and alpha(3) subunits. J Biol Chem 1996;271:27902–11.
[2] Auld DS, Kornecook TJ, Bastianetto S, Quirion R. Alzheimer's disease and the basal forebrain cholinergic system: relations to [beta]amyloid peptides, cognition, and treatment strategies. Prog Neurobiol 2002;68:209–45.
[3] Baraban SC, Tallent MK. Interneuron diversity series: interneuronal neuropeptides—endogenousregulatorsofneuronalexcitability.Trends Neurosci 2004;27:135–42.
[4] Bast T, Zhang W-N, Fledon J. Hyperactivity, decreased startle reactivity, and disrupted prepulse inhibition following disinhibition of the rat ventral hippocampus by the GABAA receptor antagonist picrotoxin. Psychopharmacology 2001;156:225–33.
[5] Billings LM, Oddo S, Green KN, McGaugh JL, LaFerla FM. Intraneuronal A[beta] causes the onset of early Alzheimer's disease-related cognitive deficits in transgenic mice. Neuron 2005;45:675–88.
[6] Blanchard V, Moussaoui S, Czech C, Touchet N, Bonici B, Planche M, et al. Time sequence of maturation of dystrophic neurites associated with A[beta] deposits in APP/PS1 transgenic mice. Exp Neurol 2003;184:247–63.
[7] BlascoB,AvendanoC,CavadaC.Astereologicalanalysisofthelateral geniculate nucleus in adult Macaca nemestrina monkeys. Vis Neurosci 1999;16:933–41.
[8] Bouilleret V, Loup F, Kiener T, Marescaux C, Fritschy JM. Early loss of interneurons and delayed subunit-specific changes in GABA(A)receptor expression in a mouse modelofmesialtemporallobeepilepsy. Hippocampus 2000;10:305–24.
[9] Bouilleret V, Schwaller B, Schurmans S, Celio MR, Fritschy JM. Neurodegenerative and morphogenic changes in a mouse model of temporal lobe epilepsy do not depend on the expression of the calciumbinding proteins parvalbumin, calbindin, or calretinin. Neuroscience 2000;97:47–58.
[10] Casas C, Sergeant N, Itier JM, Blanchard V, Wirths O, van der Kolk N, et al. Massive CA1/2 neuronal loss with intraneuronal and N-terminal truncated A{beta}42 accumulation in a novel Alzheimer transgenic model. Am J Pathol 2004;165:1289–300.
[11] Chan-Palay V, Lang W, Allen YS, Haesler U, Polak JM. Cortical neurons immunoreactive with antisera against neuropeptide Y are altered in Alzheimer's-type dementia. J Comp Neurol 1985;238: 390–400.

[12] Cossart R, Dinocourt C, Hirsch JC, Merchan PA, De Felipe J, Ben Ari Y, et al. Dendritic but not somatic GABAergic inhibition is decreased in experimental epilepsy. Nat Neurosci 2001;4:52–62.
[13] DaviesP,KatzmanR,TerryRD.Reducedsomatostatin-likeimmunoreactivity in cerebral cortex from cases of Alzheimer disease and Alzheimer senile dementa. Nature 1980;288:279–80.
[14] Davis KL, Mohs RC, Marin DB, Purohit DP, Perl DP, Lantz M, et al. Neuropeptide abnormalities in patients with early Alzheimer disease. Arch Gen Psychiatry 1999;56:981–7.
[15] Dinocourt C, Petanjek Z, Freund TF, Ben Ari Y, Esclapez M. Loss of interneurons innervating pyramidal cell dendrites and axon initial segments in the CA1regionofthehippocampusfollowing pilocarpineinduced seizures. J Comp Neurol 2003;459:407–25.
[16] Dorph-Petersen KA, Nyengaard JR, Gundersen HJG. Tissue shrinkage and unbiased stereological estimation of particle number and size. J Microsc 2001;204:232–46.
[17] Dumont M, Strazielle C, Staufenbiel M, Lalonde R. Spatial learning and exploration of environmental stimuli in 24-month-old female APP23 transgenic mice with the Swedish mutation. Brain Res 2004;1024:113–21.
[18] Floden AM, Li S, Combs CK. {beta}-Amyloid-stimulated microglia induceneurondeathviasynergisticstimulationoftumornecrosisfactor {alpha} and NMDA receptors. J Neurosci 2005;25:2566–75.
[19] FreundTF,BuzsakiG.Interneuronsofthehippocampus.Hippocampus 1996;6:347–470.
[20] GeorgM,ArneM,FlemmingJ.StereologicalcellcountsofGABAergic neurons in rat dentate hilus following transient cerebral ischemia. Exp Brain Res 2001;141:380–8.
[21] Gulledge AT, Stuart GJ. Excitatory actions of GABA in the cortex. Neuron 2003;37:299–309.
[22] Harney SC, Jones MV. Pre- and postsynaptic properties of somatic and dendritic inhibition in dentate gyrus. Neuropharmacology 2002;43:584–94.
[23] Hock BJ, LambBT.Transgenic mouse models of Alzheimer's disease. Trends Genet 2001;17:S7–12.
[24] Ida N, Hartmann T, Pantel J, Schroder J, Zerfass R, Forstl H, et al. Analysis of heterogeneous beta A4 peptides in human cerebrospinal f luid and blood by a newly developed sensitive Western blot assay. J Biol Chem 1996;271:22908–14.
[25] JinnoS,AikaY,FukudaT,KosakaT.QuantitativeanalysisofGABAergic neurons in the mouse hippocampus, with optical disector using confocal laser scanning microscope. Brain Res 1998;814:55–70.
[26] Jinno S, Kosaka T. Patterns of colocalization of neuronal nitric oxide synthase and somatostatin-like immunoreactivity in the mouse hippocampus: quantitative analysis with optical disector. Neuroscience 2004;124:797–808.
[27] JinnoS,AikaY,FukudaT,KosakaT.QuantitativeanalysisofGABAergic neurons in the mouse hippocampus, with optical disector using confocal laser scanning microscope. Brain Res 1998;814:55–70.
[28] KlausbergerT,MagillPJ,MartonLF,RobertsJD,CobdenPM,Buzsaki G, et al. Brain-state- and cell-type-specific firing of hippocampal interneurons in vivo. Nature 2003;421:844–8.

[29] Klausberger T, Marton LF, Baude A, Roberts JD, Magill PJ, Somogyi P. Spike timing of dendrite-targeting bistratified cells during hippocampal network oscillations in vivo. Nat Neurosci 2004;7: 41–7.
[30] Lowry OH, Rosebrough NJ, Farr AL, Randall RJ. Protein measurement with the Folin phenol reagent. J Biol Chem 1951;193: 265–75.
[31] LuT,PanY,KaoSY,LiC,KohaneI,ChanJ,etal.Generegulationand DNAdamage in the ageing human brain. Nature 2004;429:883–91.
[32] Lyness SA, Zarow C, Chui HC. Neuron loss in key cholinergic and aminergic nuclei in Alzheimer disease: a meta-analysis. Neurobiol Aging 2003;24:1–23.
[33] Maccaferri G, Roberts JDB, Szucs P, Cottingham CA, Somogyi P. Cell surface domain specific postsynaptic currents evoked by identif iedGABAergicneuronesinrathippocampusinvitro.JPhysiolLondon 2000;524:91–116.
[34] Maccaferri G, Lacaille JC. Interneuron diversity series: hippocampal interneuron classifications—making things as simple as possible, not simpler. Trends Neurosci 2003;26:564–71.
[35] Mattson MP. Pathways towards and away from Alzheimer's disease. Nature 2004;430:631–9.
[36] Matyas F, Freund TF, Gulyas AI. Immunocytochemically defined interneuron populations in the hippocampus of mouse strains used in transgenic technology. Hippocampus 2004;14:460–81.
[37] NilssonCL,BrinkmalmA,MinthonL,BlennowK,EkmanR.Processing of neuropeptide Y, galanin, and somatostatin in the cerebrospinal f luidofpatientswithAlzheimer'sdiseaseandfrontotemporaldementia. Peptides 2001;22:2105–12.
[38] Palop JJ, Jones B, Kekonius L, Chin J, Yu GQ, Raber J, et al. Neuronal depletion of calcium-dependent proteins in the dentate gyrus is tightly linked to Alzheimer'sdisease-related cognitive deficits. Proc Natl Acad Sci USA 2003;100:9572–7.
[39] Price DL, Tanzi RE, Borchelt DR, Sisodia SS. Alzheimer's disease: genetic studies and transgenic models. Ann Rev Genet 1998;32:461–93.
[40] Rissman RA, Mishizen-Eberz AJ, Carter TL, Wolfe BB, De Blas AL, Miralles CP, et al. Biochemical analysis of GABAA receptor subunits [alpha]1, [alpha]5, [beta]1, [beta]2 in the hippocampus of patients with Alzheimer's disease neuropathology. Neuroscience 2003;120:695–704.
[41] Ruano D, Araujo F, Revilla E, Vela J, Bergis O, Vitorica J. GABA(A) and alpha-amino-3-hydroxy-5-methylsoxazole-4-propionate receptors are differentially affected by aging in the rat hippocampus. J Biol Chem 2000;275:19585–93.
[42] Saito T, Iwata N, Tsubuki S, Takaki Y, Takano J, Huang SM, et al. Somatostatin regulates brain amyloid [beta] peptide A[beta]42 through modulation of proteolytic degradation. Nat Med 2005;11:434–9.
[43] Schmitz C, Rutten BPF, Pielen A, Schafer S, Wirths O, Tremp G, et al. Hippocampal neuron loss exceeds amyloid plaque load in a transgenic mousemodelofAlzheimer'sdisease.AmJPathol2004;164:1495–502.
[44] Selkoe DJ. Alzheimer's disease is a synaptic failure. Science 2002;298:789–91.
[45] Sik A, Penttonen M, Ylinen A, Buzsaki G. Hippocampal CA1 interneurons: an in vivo intracellular labeling study. J Neurosci 1995;15:6651–65.
[46] Sloviter RS, Zappone CA, Harvey BD, Bumanglag AV, Bender RA, Frotscher M. Dormant basket cell hypothesis revisited: relative vulnerabilities of dentate gyrus mossy

cells and inhibitory interneurons after hippocampal status epilepticus in the rat. J Comp Neurol 2003;459:44–76.
[47] Tamas G, Szabadics J, Somogyi P. Cell type- and subcellular positiondependent summation of unitary postsynaptic potentials in neocortical neurons. J Neurosci 2002;22:740–7.
[48] Van Dam D, D'Hooge R, Staufenbiel M, Van Ginneken C, Van Meir F, De Deyn PP. Age-dependent cognitive decline in the APP23 model precedes amyloid deposition. Eur J Neurosci 2003;17:388–96.
[49] Vela J, Gutierrez A, Vitorica J, Ruano D. Rat hippocampal GABAergic molecular markers are differentially affected by ageing. J Neurochem 2003;85:368–77.
[50] VelaJ,VitoricaJ, RuanoD.RapidPCR-mediatedsynthesisofcompetitor molecules for accurate quantification of beta(2) GABA(A) receptor subunit mRNA. Brain Res Brain Res Protoc 2001;8:184–90.
[51] Walsh DM, Klyubin I, Fadeeva JV, Cullen WK, Anwyl R, Wolfe MS, et al. Naturally secreted oligomers of amyloid [beta] protein potently inhibit hippocampal long-term potentiation in vivo. Nature 2002;416:535–9.
[52] West MJ, Coleman PD, Flood DG, Troncoso JC. Differences in the pattern of hippocampalneuronallossinnormalageingandAlzheimer's disease. Lancet 1994;344:769–72.
[53] West MJ, Kawas CH, Stewart WF, Rudow GL, Troncoso JC. HippocampalneuronsinpreclinicalAlzheimer'sdisease.NeurobiolAging 2004;25:1205–12.
[54] Wirths O, Multhaup G, Bayer TA. A modified "beta"-amyloid hypothesis: intraneuronal accumulation of the "beta"-amyloid peptide—the f irst step of a fatal cascade. J Neurochem 2004;91:513–20.

Figures legends

Figure. 1. The expression of SOM and NPY neuropeptide mRNAs decreased early in the life-span of PS1 × APP double tg mice. The expression of both SOM (A) and NPY (B) mRNAs has been quantified in a large population (n = 25–30) of WT, PS1 and PS1 × APP tg mice of a wide age range (from 2- to 18-month-old). The expression of these two neuropeptides decreased early (4–6 months of age) only in the PS1 × APP tg mice. At older ages (18 months) the levels of both neuropeptide mRNAs were also decreased in PS1 single tg mice. (C) There was a linear relationship between the expression of SOM and NPY in all ages and animal groups. These changes in expression were not due to a generalized decrease in the PS1 × APP mice since the expression of other GABAergic marker, such as PV, was not changed in the same mice groups (inset). (D) The expression of SOM was analyzed in 6-month-old WT, PS1, APP and PS1 × APP littermates. As shown, at this specific age, the expression of this neuropeptide was significantly reduced (ANOVA $F(3,20) = 20.51$, $p = 0.0001$; Scheffe $p < 0.05$) exclusively in PS1 × APP double tg mice. *Significant difference from age matched WT mice; ANOVA followed by Scheffe test, $p < 0.05$.

Figure. 2. The number of SOM-immunopositive cells is reduced in 6-month-old PS1 × APP mice hippocampus. (A–C) Light microscopic images of SOM-immunolabeled hippocampal sections through CA1 subfield (A1, B1 and C1) and dentate

gyrus (A2, B2 and C2) of WT (A1 and A2), PS1 (B1 and B2) and PS1 × APP (C1 and C2) mice at 6 months of age. The number of SOM-positive cells (arrows) in the stratum oriens of CA1 and in the hilus of the dentate gyrus was reduced in PS1 × APP mice compared to PS1 and WT mice. The number of SOM interneurons remained unchanged between PS1 tg and WT mice. (D) Light microscopic images of PV immunostaining in CA1 subfield of WT (D1), PS1 (D2) and PS1 × APP (D3) at 6 months of age. No differences were detected in the immunolabeling pattern of PS1 × APP compared to PS1 or WT animals. (E) Stereological quantification of SOM-immunoreactive cell densities (cell/mm^3) in CA1, CA2–3 and dentate gyrus of 6-month-old WT, PS1 and PS1 × APP mice (n = 6/group). There were significant (*ANOVA $F(2,15) = 8.43$ $p = 0.002$; $F(2,15) = 11.38$, $p = 0.001$; $F(2,15) = 7.2$, $p = 0.00$ 2 for CA1, CA2–3 and DG) decreases in the SOM-positive numerical density in all hippocampal fields of double tg mice compared with WT or PS1 groups (Scheffe $p < 0.05$). Insert shows stereological quantification of CA1 pyramidal cells and no statistical differences were found in PS1 × APP mice compared to WT or PS1 mice. SO, stratum oriens; SP, stratum pyramidale; G, granular cell layer of dentate gyrus; H: hilus. Scale bar: 50 μm.

Figure. 3. Loss of SOM/NPY-containing interneurons in 6-month-old PS1 × APP tg mice hippocampus. (A–C) Immunofluorescent double-labeled confocal laser scanning images, representative of five different mice per group, for neuropeptides NPY (A1, B1 and C1) and SOM (A2, B2 and C2) in the dentate gyrus of 6-month-old WT (A1–3), PS1 (B1–3) and PS1 × APP (C1–3) mice. The corresponding merged images showed that the density of hilar interneurons containing both neuropeptides (arrows) is clearly reduced in PS1 × APP mice (C3) compared with PS1 (B3) and WT (A3). No apparent differences in the number of double labeled somata were found between WT and PS1 mice. Merged images showed that most of the interneurons co-localize SOM and NPY peptides. h, hilus; g, granular cell layer. Scale bar: 50 μm.

Figure. 4. The SOM and NPY expression was specifically altered in 6-month-old PS1 × APP double tg mice. The expression of multiple GABAergic (A), glutamatergic and cholinergic (B) neurotransmission markers was assayed in a new population of 6-month-old WT and PS1 × APP tg mice (n = 18). From a total of 22 different mRNAs quantified, only the expression of SOM and NPY mRNAs was significantly decreased, as compared with the age matched WT mice (two-tailed t-test, $t = 5.96$, $p < 0.0001$ and $t = 4.64$, $p < 0.0001$ for SOM and NPY, respectively).

Figure. 5. Comparison of the density of SOM-NeuN immunopositive interneurons in the CA1 subfield between 6-month-old wildtype and PS1 × APP mice. (A and B) Light microscopic images of double immunolabeling with SOM (blue) and NeuN (brown) in CA1 subfield of WT (A) and PS1 × APP tg (B) mice. A reduced density of stratum oriens interneurons (NeuN-positive cells) as well as SOM-immunoreactive cells (double labeled cells; arrows) was found in PS1 × APP mice compared with WT. (C) Stereological quantification of NeuN-positive cells and SOM-positive cells in CA1 stratum oriens of WT, PS1 and PS1 × APP demonstrated a significant (ANOVA $F(2,10) = 8.1$, $p = 0.015$; $F(2,10) = 6.70$, $p = 0.019$) decrease of total interneurons and SOM-containing interneurons, respectively, in PS1 × APP mice (n = 4) compared to WT (n = 4) and PS1 (n = 4) mice. The loss in the SOM-positive cell number (calculated by the difference in the SOM-positive cell number between WT and

PS1 × APP) was similar to the loss of NeuN labeled cells. SO, stratum oriens; SP, stratum pyramidale. Scale bar: 25 μm.

Figure. 6. The SOM-immunolabeled axonal field in stratum lacunosum moleculare is reduced in 6-month-old PS1 × APP mice hippocampus. (A and B) Light microscopic images of SOM-immunolabeled hippocampal CA1 subfield of 6-month-old WT (A) and PS1 × APP tg (B) mice showing the immunoreactive axonal field of SOM cells in the stratum lacunosum moleculare. The thickness of the SOM-immunoreactive axonal field was reduced in PS1 × APP mice compared with WT animals. (C) The volume (mm^3) of the SOM-immunolabeled axonal field in CA1 stratum lacunosum moleculare was significantly (*two-tailed *t*-test, see text) reduced only at caudal levels in PS1 × APP mice ($n = 3$) compared to WT ($n = 3$). The total volume measurement (including rostral + middle + caudal levels) also showed significant decrease in the double tg mice. SO, stratum oriens; SP, stratum pyramidale; SR, stratum radiatum; SLM, stratum lacunosum moleculare. Scale bar: 50 μm.

Figure. 7. The decrease in SOM and NPY expression was related to the relative abundance of Abeta peptides in 6-month-old PS1 × APP hippocampus. The production of Abeta peptides was quantified, by Western blots, in the protein fraction obtained from 23 samples of 6-month-old PS1 × APP hippocampi. (A) Representative Western blot of seven different age matched PS1 × APP mice. Equal amount of protein (2.5 μg/lane) was run in parallel and developed using the mAb 6E10. These experiments were repeated three times using different animal combinations. As shown, the amount of Abeta peptides (4.5 kDa band) varied within the different PS1 × APP mice tested. This high variation was not due to the amount of protein loaded (B). (C) Quantitative representation of the different Western blots (the Abeta signal was normalized by beta-actin). As expected, there is a large heterogeneity in the amount of Abeta peptides (closed squares). This heterogeneity was similar to that observed in the expression of SOM mRNAs (gray circles) from the same mice. The expression of SOM in WT (open circles) was included for comparative purposes. (D) Relationship between the Abeta content and the expression of SOM (gray circles) or NPY (closed squares) mRNAs from 6-month-old PS1 × APP mice. The WT values (triangles) were included for comparison. Note the difference in scales between SOM and NPY mRNAs. (E–G) Light microscopic images showing CA1 subfield of PS1APP mice hippocampus at 2 (E), 4 (F) and 6 (G) months of age immunostained with anti-beta-specific antibody 6E10. Pyramidal cell layer showed intense intracellular immunolabeling at all these ages. However, GABAergic interneurons did not appear immunolabeled. Extracellular Abeta deposits (arrows) were first detectable at 4 months of age and mostly located in the stratum oriens. The amount of extracelullar amyloid deposition increased with age. SO, stratum oriens; SP, stratum pyramidale; SR, stratum radiatum. Scale bar: 100 μm.

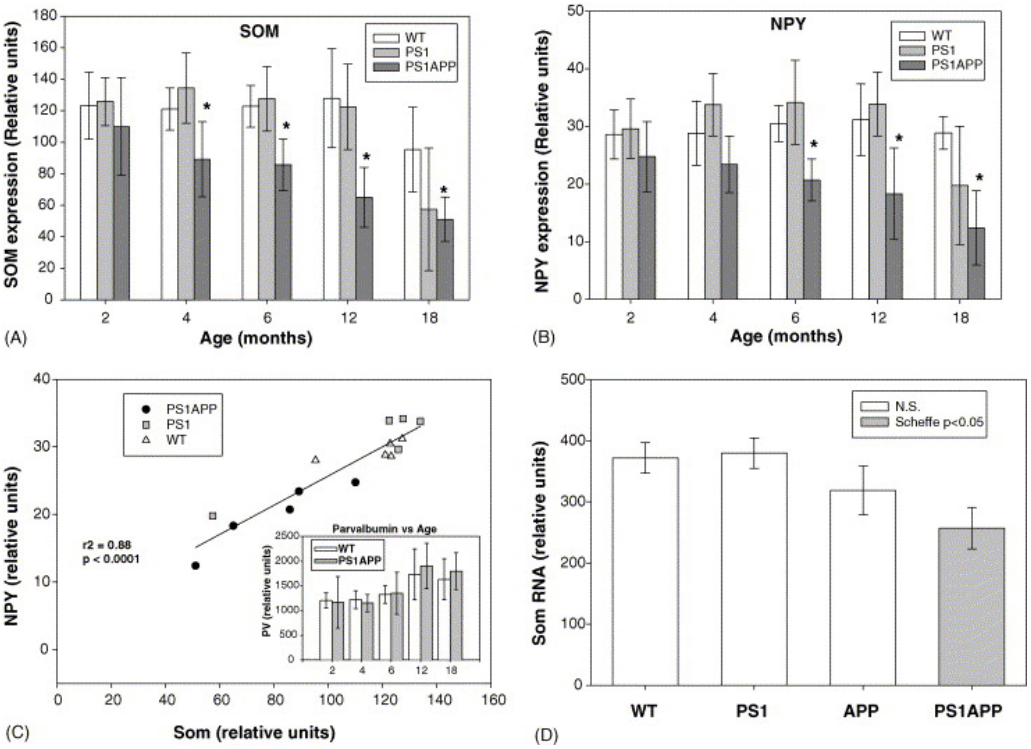
SOM
WT
PS1
PS1APP
SOM expression (Relative units)
Age (months)
(A)
NPY
NPY expression (Relative units)
(B)
PS1APP
PS1
WT
r2 = 0.88
p < 0.0001
NPY (relative units)
Som (relative units)
Parvalbumin vs Age
PV (relative units)
(C)
N.S.
Scheffe p<0.05
Som RNA (relative units)
WT
PS1
APP
PS1APP
(D)

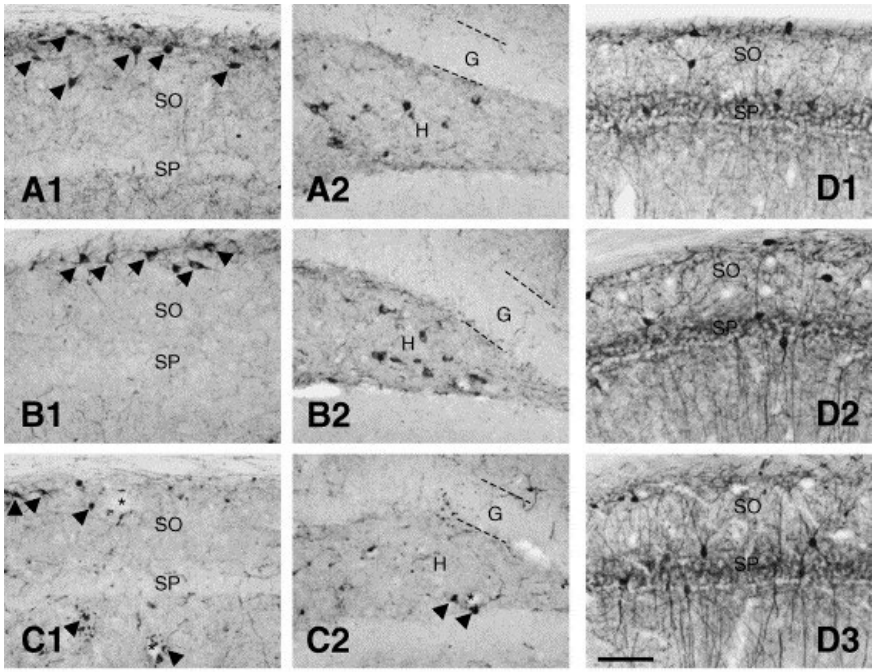
A1
SO
SP
A2
G
H
D1
SO
SP
B1
SO
SP
B2
G
H
D2
SO
SP
C1
SO
SP
C2
G
H
D3
SO
SP

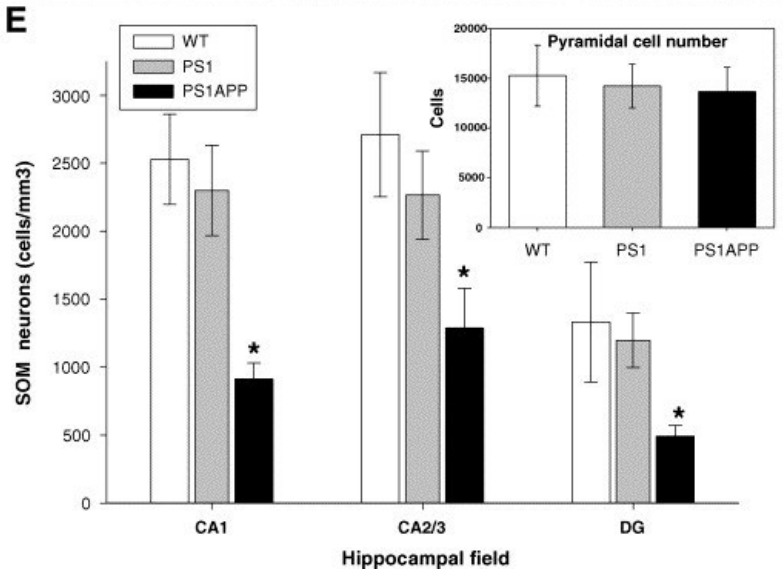
E
WT
PS1
PS1APP
SOM neurons (cells/mm3)
3000
2500
2000
1500
1000
500
0
CA1
CA2/3
DG
Hippocampal field
Pyramidal cell number
Cells
20000
15000
10000
5000
0
WT
PS1
PS1APP

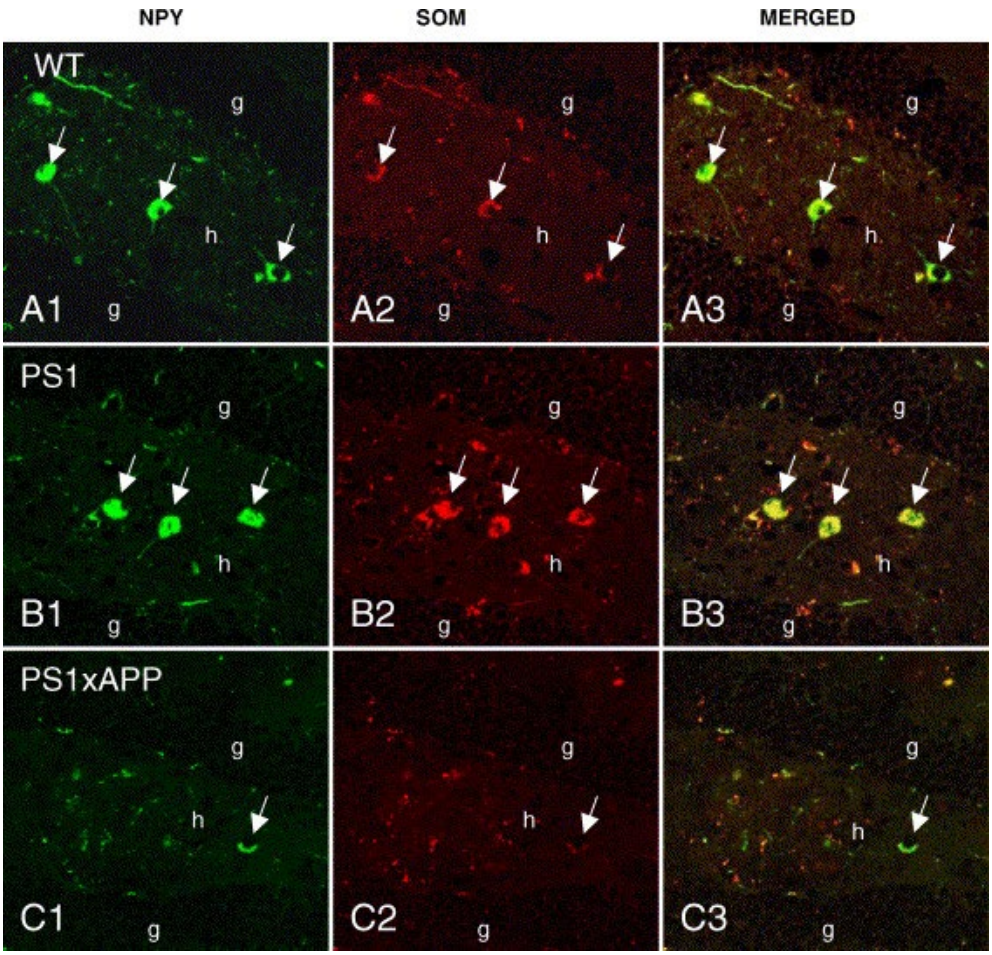
NPY
SOM
MERGED
WT
PS1
PS1xAPP
A1
A2
A3
B1
B2
B3
C1
C2
C3
g
h

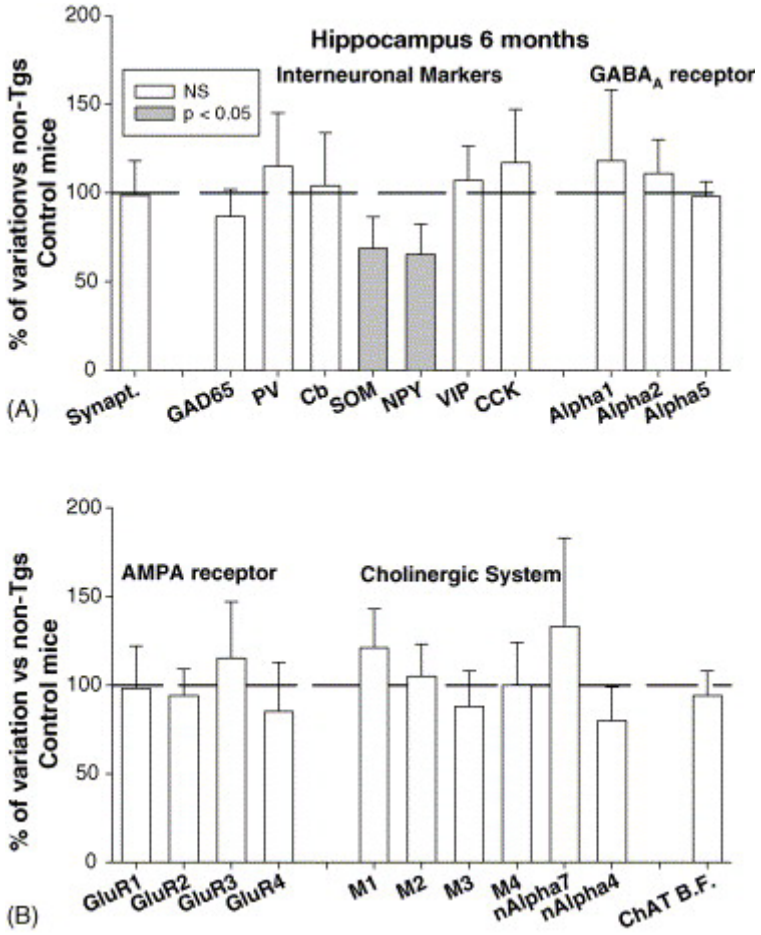
Hippocampus 6 months
Interneuronal Markers
GABA$_A$ receptor
NS
p < 0.05
% of variationvs non-Tgs Control mice
200
150
100
50
0
(A)
Synapt.
GAD65
PV
Cb
SOM
NPY
VIP
CCK
Alpha1
Alpha2
Alpha5
AMPA receptor
Cholinergic System
% of variation vs non-Tgs Control mice
(B)
GluR1
GluR2
GluR3
GluR4
M1
M2
M3
M4
nAlpha7
nAlpha4
ChAT B.F.

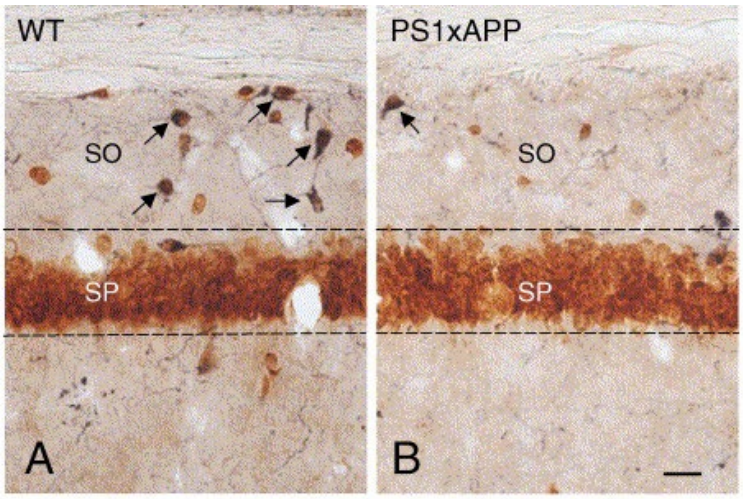

C

	Numerical Density (cells/mm3)			
			Difference from WT	
	NeuN	SOM	NeuN	SOM
WT	14.244 ± 2847	8.269 ± 1939		
PS1	13.644 ± 2462	7.852 ± 1563	600 ± 2462	418 ± 1563
PS1xAPP	**8.351 ± 1137[a]**	**3.154 ± 1560[a]**	**5.893 ± 222**	**5.114 ± 695**

10-12 sections per mouse and 4 mice per group
[a] Scheffe $p<0.05$

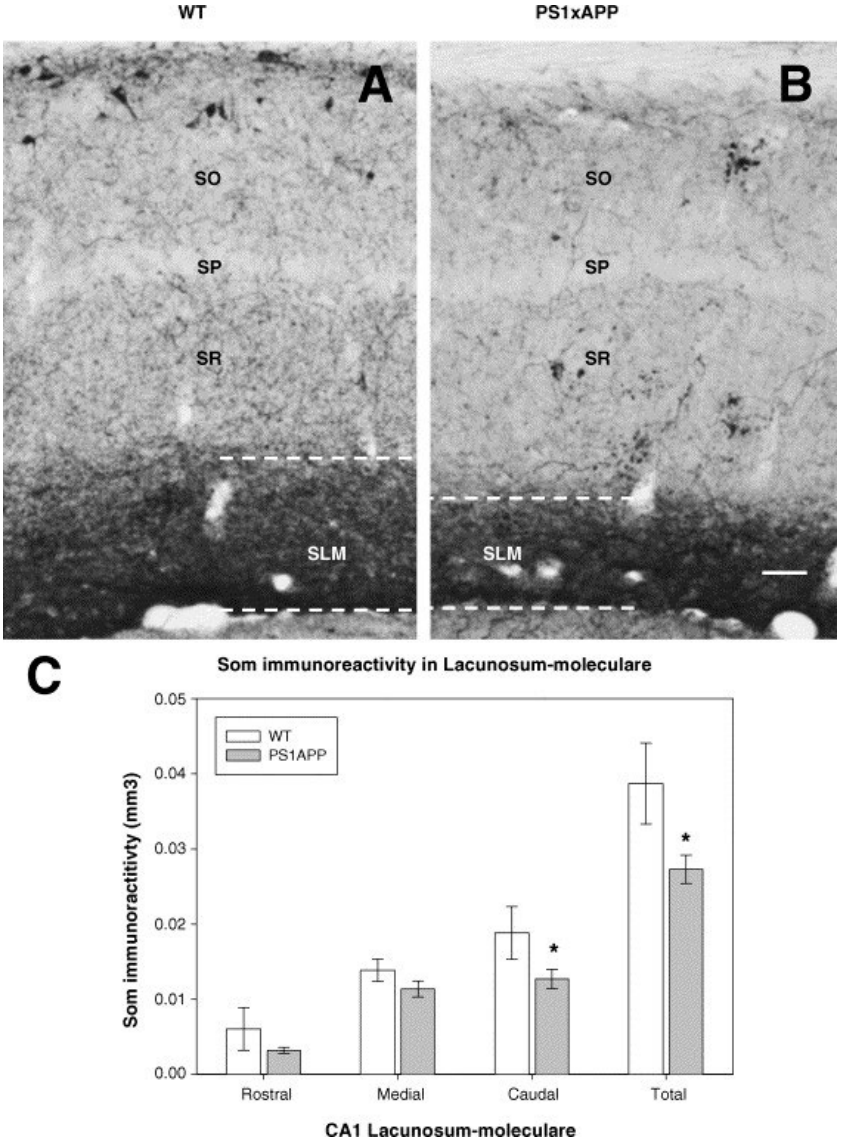
WT
PS1xAPP
A
B
SO
SP
SR
SLM
SO
SP
SR
SLM
C
Som immunoreactivity in Lacunosum-moleculare
WT
PS1APP
Som immunoractitivty (mm3)
0.05
0.04
0.03
0.02
0.01
0.00
*
*
Rostral
Medial
Caudal
Total
CA1 Lacunosum-moleculare

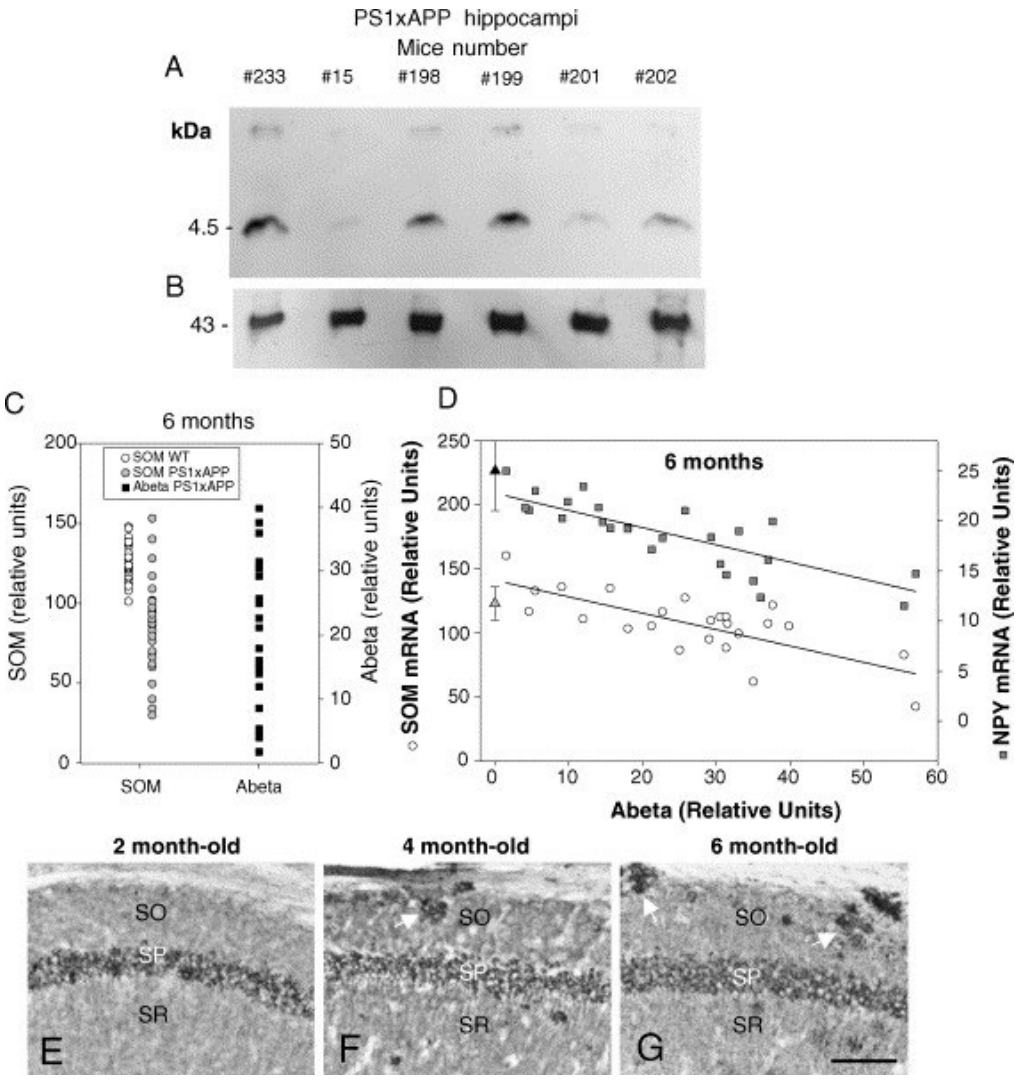
PS1xAPP hippocampi
Mice number
A
#233
#15
#198
#199
#201
#202
kDa
4.5
B
43
C
6 months
SOM WT
SOM PS1xAPP
Abeta PS1xAPP
SOM (relative units)
Abeta (relative units)
SOM
Abeta
D
6 months
SOM mRNA (Relative Units)
NPY mRNA (Relative Units)
Abeta (Relative Units)
2 month-old
4 month-old
6 month-old
SO
SP
SR
E
F
G